ANNUAL REVIEWS

Annual Review of Biophysics

Graphene and Two-Dimensional Materials for Biomolecule Sensing

Deependra Kumar Ban[1,2] and Prabhakar R. Bandaru[1,3]

[1]Department of Mechanical Engineering, University of California, San Diego, California, USA

[2]Current affiliation: Keck Graduate Institute, Claremont, California, USA

[3]Program in Materials Science & Engineering, University of California, San Diego, California, USA; email: pbandaru@ucsd.edu

Annu. Rev. Biophys. 2023. 52:487–507

First published as a Review in Advance on February 15, 2023

The *Annual Review of Biophysics* is online at biophys.annualreviews.org

https://doi.org/10.1146/annurev-biophys-111622-091121

Keywords

specific surface area, SSA, density of states, DOS, field effect transistor, FET, impedance models, defects, standardization

Abstract

An ideal biosensor material at room temperature, with an extremely large surface area per unit mass combined with the possibility of harnessing quantum mechanical attributes, would be comprised of graphene and other two-dimensional (2D) materials. The sensing of a variety of sizes and types of biomolecules involves modulation of the electrical charge density of (current through) the 2D material and manifests through specific components of the capacitance (resistance). While sensitive detection at the single-molecule level, i.e., at zeptomolar concentrations, may be achieved, specificity in a complex mixture is more demanding. Attention should be paid to the influence of inevitably present defects in the 2D materials on the sensing, as well as calibration of obtained results with acceptable standards. The consequent establishment of a roadmap for the widespread deployment of 2D material–based biosensors in point-of-care platforms has the potential to revolutionize health care.

Contents

1. INTRODUCTION

The all-surface characteristic of a two-dimensional (2D) material, such as graphene, has been of much utility for propagating a new class of biosensors. Such an approach provides advantages both (*a*) related to a classical influence of an extremely large surface area–to-volume ratio, given the atomic thickness of the 2D material, and (*b*) from a quantum mechanics (QM) perspective—where the tunability of carrier density, as well as the discreteness of energy levels, may play a role and may be harnessed for new sensing modalities. With respect to the first attribute, the specific surface area (SSA) of one side of single-layer graphene has been estimated to be very large, at approximately 1,315 m^2/g (102) based on the relatively short C-C bond length of 0.142 nm, and thus orders of magnitude larger than that of porous materials (79). Additionally, there are no diffusional and mass transfer limitations to sensing (45). Such attributes extend to other 2D materials as well, e.g., MoS_2, with SSA values ranging from 100 m^2/g to 400 m^2/g (149), albeit with active sites associated mostly on edges and defects (142). However, there are corresponding disadvantages to the large SSA as well. For instance, extreme sensitivity of the material to the environment could arise at the expense of specific monitoring of species. A QM perspective, with energy level–specific sensing, could be useful in addressing this issue and motivate future efforts at enhancing the specificity.

This review aims to elucidate the scientific rationale behind the utility of 2D materials for biomolecule sensors, with an emphasis on graphene. The applications are focused on external and in vitro usage, given the toxicological implications of carbon nanostructures (39, 60, 114). While alternate derivatives, such as reduced graphene oxide (rGO) (27, 127), have been touted for ultra-sensitive (26) biomolecule sensors (71, 91), mainly due to their ease of synthesis as well as their low cost, they have been difficult to characterize on a fundamental basis. Moreover, the quality

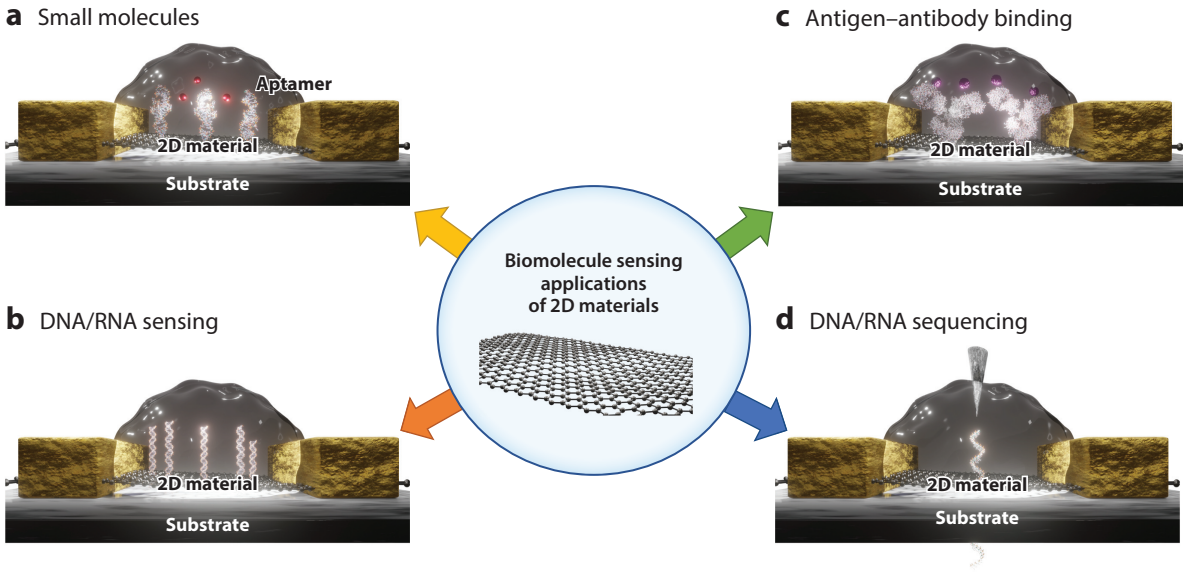

Figure 1

A schematic summary of the application of 2D material–based biosensing for (*a*) small-molecule detection using aptamers, (*b*) DNA or RNA sensing, (*c*) virus particle or protein detection through antigen–antibody binding, and (*d*) derived nanopore-based genomic sequencing.

is rather poor for such derivatized materials. For example, at room temperature, the rGO has an electrical carrier mobility of at most 300 cm^2/V.s (137), two orders of magnitude smaller in comparison to graphene, which has mobility approaching 50,000 cm^2/V.s (12), when both materials are synthesized through industrial-scale methods, i.e., through the Hummers method (52, 85) (involving the addition of potassium permanganate to a solution of graphite, sodium nitrate, and sulfuric acid) for the graphene oxide (GO) and chemical vapor deposition for the graphene films. Consequently, this review focuses on graphene. Moreover, it is often seen that, even in purportedly uniform graphene films, there are inevitable defects (9) that modulate the sensor characteristics. It is thus important to emphasize the state-of-the-art understanding and usage of graphene and how it could be better adapted for high-sensitivity as well as high-specificity sensing.

A general principle of biosensing that has been most adopted for 2D materials (for a brief summary, see **Figure 1**) is the modulation of the electrical current in the material-constituted device, such as the field effect transistor (FET) (6), facilitated by the interaction of the biomolecule with the surface.

2. BIOMOLECULE (OR ANALYTE)–GRAPHENE SURFACE INTERACTIONS

Considering graphene as a prototype, **Figure 2** shows that the related crystal structure is composed of two sublattices of carbon atoms with different local environments. In plane, the C atoms are associated through σ-bonding from the overlap of hybridized sp^2 orbitals, while the p_z orbitals are perpendicular to the plane (62). Given the stability of the σ-bonds, the modulation of the electrical conductivity of the graphene by an analyte must occur through interaction with the p_z orbitals, which are relatively localized (**Figure 2*a***). Moreover, considering the hydrophobic character of the graphene resulting from the high in-plane surface energy, organic moieties would be preferred for π–bonding-related cross-plane linkage.

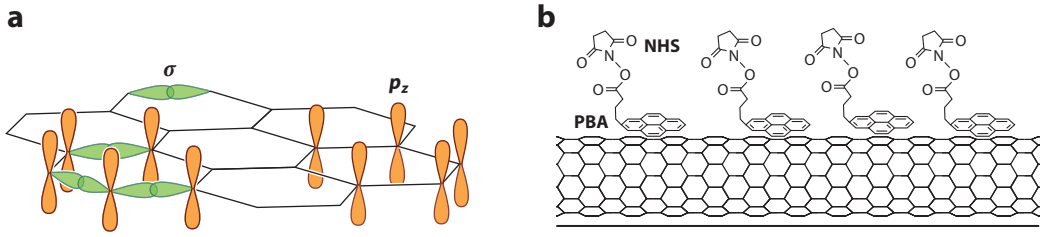

Figure 2

(*a*) The σ-bonding between the C atoms is associated with the in-plane rigidity, while the out-of-plane p_z orbitals are relatively localized on the atoms, with overlap through covalent π-bonds. The interaction of the analytes with a defect-free graphene surface primarily occurs through the p_z orbitals and would be related to the π-bonding. (*b*) An example of a typical graphene functionalization scheme with a 1-pyrenebutyric acid (PBA) linker–N-hydroxy succinimide (NHS) ester connector moiety anchored noncovalently onto the surface. The amine-reactive NHS may be deployed for environment-sensitive nucleic acid detection. Panel *b* adapted with permission from Reference 25; copyright 2001 American Chemical Society.

Generally, linkage to the graphene surface atoms and consequent modulation of the in-plane electrical properties, while minimally perturbing the surface, may be accomplished through noncovalent functionalization (25), as indicated in **Figure 2*b***. A related example, the 1-pyrenebutyric acid (PBA) linker–N-hydroxy succinimide (NHS) ester connector, is a commonly utilized surface functionalization linker chemistry (97) for modulating the electrical characteristics of graphene biosensors (84).

It thus seems to be broadly indicated that the overlap of the π-bonding, e.g., from the benzene-/phenyl-related rings in organic moieties with that of the graphene, is necessary. The analyte would then be immobilized onto the connector–linker moiety, and the subsequent interaction would consequently perturb the electrical property of the 2D material and be transduced into the identity of the analyte. Noncovalent binding that incorporates electrostatic interactions is also relevant for compound 2D materials such as MoS_2 or WS_2 (82) and is expected to be dominant for smaller biomolecules but less well defined for larger molecules, such as DNA. However, the chemical factors are not sufficient to explain all aspects of these interactions, and the mechanical rigidity must also be considered, e.g., the tighter binding of low-persistence-length single-stranded DNA (110) to graphene (73) or MoS_2 (77) surfaces compared to stiffer double-stranded DNA.

Alternately, when the 2D material is chemically modified, e.g., as in GO, the pendant modifiers on the substrate (64) could directly link to the analyte, such as DNA (83) or streptavidin (81). It was noted that the DNA would be adsorbed onto the GO surface through hydrogen bonding, in addition to $\pi-\pi$ stacking. The tetrameric configuration of the four streptavidin-binding biotinylated molecules with high affinity and selectivity has been extensively utilized in immunoassays (36). In this case, both primary and secondary bonding may be involved. However, useful sensors, e.g., an rGO-based enzyme-modified FET for monitoring neurotransmitter (acetylcholine)–inhibitor (acetylcholinesterase) kinetics relevant to Alzheimer's disease (22), have been deployed, and such studies provide motivation for further investigation.

In summary, noncovalent functionalization is the preferred basis for preserving the high surface area and lower-dimensional characteristic of 2D materials. Consequently, the utilization of access, as well as unique attributes such as quantum capacitance, would be relevant.

2.1. Biomolecule Sensing Modalities

Current research aims to understand the adsorption of biomolecule moieties and subsequent detection and transduction on an atomistic or microscopic, as well as at the mesoscopic, level. Such

consideration is relevant given that biomolecular systems of practical interest cover a molecular weight range over six orders of magnitude, from 1 Da—related to approximately the mass of a H atom—to millions of Da for proteins. Given that the areal density of carbon atoms in graphene is $3.82 \times 10^{15}/\text{cm}^2$ (105), and that the noncovalent or van der Waals interaction occurs at a spacing of the order of 0.335 nm, there would be significant scope for attachment of the biomolecule. However, the kinetic aspects related to the binding and unbinding of the moieties must be considered as well.

A useful metric for gauging the extent of binding interaction of a biomolecule with the substrate or surface would be the equilibrium dissociation constant (K_D)—the ratio of the unbinding-related backward rate constant (K_{off}) to the binding-related forward rate constant (K_{on}) (96). A smaller (larger) K_D implies stronger (weaker) attraction. The K_D is interpreted as the concentration at which half of the binding sites are occupied at equilibrium. A low (high) affinity is typically related to a K_D larger (smaller) than 100 μM (100 nM), provided that adequate controls to ensure equilibrium and invariance under titration are ensured (59). Equilibration may be indicated by varying the biomolecule incubation time and checking that the obtained results do not change with time. While a K_D of the order of 1 μM needs equilibration times of the order of seconds, the determination of a smaller K_D, e.g., in the 1 nM range, may need up to hours. It is thus apparent that an adequate concentration of the analyte with respect to the K_D must be present, and this concentration is relevant for accurate determination of the sensitivity of the biomolecule sensor.

Thus, the range of biomolecules that may be sensed encompasses trace metals, such as As, Cu, Fe, Hg, Pb, and Zn, which play significant roles in animal health, as well as in medical diagnostics (17) and drug testing (4, 26). However, there are potential problems: Nonspecific interaction on the graphene surface may induce variable sensor response (63, 131), and probing of the larger systems also involves disordered adsorption with a complex energy landscape. In this context, amino acids, with an average molecular weight of 100 Da, provide a relevant point of comparison between the smaller and the larger biomolecule systems and would be relevant to peptides (constituted from 2 to 50 amino acids) and proteins (typically with greater than 50 amino acids). For instance, sampling of specific peptide regions would provide insight into larger systems (119, 147). Investigations into the binding of the acids, and subsequently bases, onto graphene surfaces are expected to yield insights into the binding of macroscopic configurations.

2.2. Adsorption of Amino Acids onto Graphene

A comprehensive computational study of the noncovalent interactions of all 20 amino acids with graphene surfaces in aqueous solutions indicated enhanced binding correlated with the presence of "flat (or compact) side chain groups" (51, p. 3220). Molecular dynamics (MD) simulations using specific force fields were used for such analyses. For instance, the graphene surface was described as a rigid dipole, while the amino acid adsorbates in aqueous environments are modeled through the CHARMM (Chemistry at Harvard Molecular Mechanics) set (**https://projects.iq.harvard.edu/karplusgroup/charmm**) (for a list of amino acids, see **Supplemental Figure R1**). There is an implicit trade-off between the rigor of the described interactions with respect to the computational complexity and the cost, and many of the simulations still need to be experimentally verified in detail.

Supplemental Material >

The affinity of the amino acids was monitored through the free energy of adsorption: $\Delta G_{\text{ads}} = RT \ln (K_D)$, where R is the gas constant (8.31 J/mol.K), and T is the temperature. The ΔG_{ads} was indicated to be of the order of 20 kJ/mol (approximately 0.2 eV and corresponding to a K_D of approximately 300 μM) for charged or polar acids, e.g., arginine (Arg), glutamine (Gln), or tyrosine (Tyr), and a factor of up to 10 smaller for nonpolar acids, e.g., isoleucine (Ile), valine (Val),

or proline (Pro). A variety of approximate correlations have been indicated for greater adsorption onto the graphene surface, such as (*a*) lower amino acid mass and less bulky character, (*b*) increased hydrophobicity (69), and (*c*) increased aromatic character. Such aspects have been indicated to be important in understanding the adsorption of the amino acids, such as Arg, Trp, and Tyr, onto gold surfaces (51). It is known, for instance, from studies on molecular electronics (121) that the local electronic configuration of the electrodes, as well as the conformation of the functionalizing agent (or anchor) of the analyte, plays a significant role in modulating the obtained conductivity.

It is well known that the 20 amino acids are encoded by a triplet of nucleotides, which in turn are constituted from the bases or nucleobases, i.e., adenosine (A), thymine (T), uracil (U), cytosine (C), and guanine (G). The bases are also the building blocks of DNA and RNA, and their individual coupling with the 2D materials would be relevant to a better understanding of the interaction of the aggregate amino acids. Recent hypotheses that RNA–peptide coevolution is the basis for the origin of life (78), as well as the possibility of generating functional nanomaterials (106), provide further motivation for the study of such interactions.

2.3. Adsorption of Nucleobases onto Graphene

A study involving the interaction of graphene with A, T, C, and G indicated that the relative binding energy of the nucleobases was in the order of G > A > C > T (130), similar to what was found in single-walled nanotubes. Such trends are in general agreement with theoretical expectations and experimental measurements (100). The related interactions of the DNA constituents cause molecule-specific (34) modulation of 2D material–based carrier mobility and conductivity, which may be used for their detection. While the large size of proteins and peptides implies the lack of an ordered placement onto the sensing surface, the design of constituent base sequences known to bind onto the surface could yield insights into amino acid–guided molecular conformations and protein–solid interactions. Studies related to the design and development of solid-binding peptides would be particularly useful.

Amino acid domains along the primary sequence of the peptides may be engineered for spatial organization onto the graphene surfaces. For instance, a computational study–based selection of a graphite-binding dodecapeptide (GrBP) with sequences exhibiting affinity to the surface was conducted (119). It was determined that replacing the Tyr with Ala (Trp) would reduce the affinity of the binding to graphite—delineating experimentally the differences between polar and nonpolar amino acids. Furthermore, the extent of ordering could be increased (diminished) by specific genetic mutations—which were also determined to control the extent of the hydrophobic (-philic) character (30). The initial disordered aggregation, followed by ordering, was monitored through atomic force microscopy, as was the change in the contact angle related to a modulation of the surface energies (57).

Such amphiphilic assembly—involving attachment of polar groups to graphene or other 2D material, e.g., MoS_2, surfaces—may then serve as a linker to many other biological moieties of interest, such as proteins, enzymes, and antibodies (147). The adhesion is still noncovalent, implying minimal perturbation of the sensing surface, with a K_D in the range of 50 nM–1 μM.

Having considered the nature of the surface and the modalities of interaction, we next indicate the principles behind the diagnostic methods typically deployed for biomolecule sensing.

3. INTERFACING OF THE ELECTRICAL CHARACTERISTICS OF GRAPHENE AND BIOMOLECULES

A common principle for biomolecule sensing seems to be based on the fact that charge from analyte on the surface influences the resultant electrical current. The current may be either of

the displacive type—as arising from a time-varying electrical field—or of the conduction type—involving the actual flow of electrical carriers (38). The former (latter) type of sensing is deployed in capacitive (transistor)-based sensing, where the 2D material forms the dielectric (conducting) channel. The extent of the current modulation would be dependent on the size as well as the conformation of the analyte.

The presence of any moiety on the surface of graphene would be expected to locally (*a*) modulate the charge density or (*b*) obstruct the electrical current. The first possibility contributes to the electrical capacitance (*C*), and the second would change the electrical resistance (*R*). Frequency-specific modulation by an applied voltage would result in electrical currents, with an in-phase component related to the *R* and an out-of-phase component related to the *C*. The device response, at a given frequency, could then be related to the time scale associated with the analyte conformation kinetics. Both two-terminal capacitors and three-terminal transistors have been deployed in biosensors and measure the impedance—a combination of the *R* and *C*—through the ratio of the applied voltage to the measured current.

3.1. Capacitance and Resistance Contributions Related to 2D Materials Interfaced with Biomolecules in Liquid Media

Analyte-based charge sensing may be accomplished through externally monitoring the *C* change through an electrical circuit. While metal–oxide and semiconductor–metal capacitors have been extensively used for simple analyte sensing, such as for ethanol or water (88), more complex biomolecular systems require more detailed analysis of all of the contributing classical and quantum capacitances (65). Such factors imply that considerations of capacitance monitoring must move far beyond the traditional viewpoint of a fixed dielectric between two metal electrodes.

From the viewpoint of classical electrostatics, the placement of a 2D material–constituted substrate in an electrolyte or buffer solution would be accompanied by a surface charge due to the relative difference of the dielectric constants ($\varepsilon = \varepsilon_o \varepsilon_r$, with ε_o as the permittivity of free space and ε_r as the relative dielectric permittivity). When the analyte-sensing surface is positive (negative), it would be surrounded by corresponding negative (positive) charge, which interacts with the analyte. The adjacent oppositely charged layers constitute a double-layer (13, 31, 46, 116) capacitance: C_{dl}. The resultant Helmholtz capacitance (per unit area), with charge stored in a layer of thickness (*d*) both internal and external to the material, would be proportional to $\sim \frac{\varepsilon}{d}$. The double-layer attribute may then be first related to an internal capacitance, i.e., the space charge capacitance, C_{SC} (43, 90, 123), arising from the screening of the ambient charge into the inner layers of the 2D material by the outer layers (2) over a distance termed the Thomas-Fermi screening length, $d_{\mathrm{T-F}} = \sqrt{\frac{\varepsilon E_F}{2\,ne^2}}$. The $d_{\mathrm{T-F}}$ is related to the span over which the electrical carriers in the 2D material (of carrier density *n*, with *e* as the elementary electron charge and Fermi energy E_{F}) exert their influence into the ambient (72). It has been noted that an atomic layer sheet, with a carrier concentration (*n*) of the order of $5 \times 10^{20}/\mathrm{cm}^3$, typical to graphene (62, 68), would not completely screen the electric fields, and a single-layer 2D material could not constitute a perfect electrode (94). There would thus always be a C_{SC} for multiple-layered 2D materials, such as few-layer graphenes, MoS_2, WS_2, and Mo_2P. Additionally, immobile surface charges (due to defects) may also contribute to the space charge and related capacitance. The large electric field at the surface (due to the potential drop over the size scale of an ion) indicates that it is necessary to consider orientational effects, e.g., of the molecules at the surface (140). Consequently, the ε_r may be considerably reduced (28) as much as an order of magnitude from the assumed bulk value, e.g., for water, from approximately 80 to as low as 4.7 for H^+/OH^- ion–2D material surfaces, which complicates our understanding of interactions with 2D material surfaces (75).

External to the surface, i.e., in the electrolyte or ambient, there would be a spread of the counteracting carriers or ions, with the resultant distribution and the surface potential (ϕ_s) variation yielding a diffusion capacitance (C_{diff}) related to the double-layer capacitance; in this case, the d would be related to both ion size and the diffuse layer thickness, as reckoned through the Debye length, $d_{\text{Debye}} = \sqrt{\frac{\varepsilon k_B T}{2(ze)^2 I^o}}$ (14). In this equation, z is the magnitude of ion charge, e.g., +1 for H^+/Na^+ and −1 for OH^-/Cl^-; k_B is the Boltzmann constant; T is the temperature; and I^o is the ambient ion concentration. It is assumed that the carrier concentration varies as $\exp(-e/k_B T)$ and that d_{Debye} is related to the length scales associated with the Poisson-Boltzmann equation (14).

A characteristic particular to low-dimensional materials (7, 8) such as graphene is the ability to tune the density of states (DOS)—the number of electronic states per unit energy. Consequently, there is a relatively larger increase (decrease) of the E_F when an electronic charge of magnitude dQ ($=e \times dn$) is added (removed) due to an applied voltage change (dV) (29). An effective quantum capacitance (C_Q) in series with the C_{dl} could be defined, considering the DOS at the E_F, as follows (9, 145): $C_Q = \frac{e \cdot dn}{(dE_F/e)} = e^2 \text{DOS}(E_F)$. A low C_Q generally indicates lack of available states that can be occupied and influences device characteristics. Broadly, a net applied change in voltage (ΔV) is related to a differential change in the E_F and would be partitioned between the 2D material (as ΔV_Q and associated with the C_Q) and the surrounding ambient or environment (ΔV_E, associated with electrostatic capacitances due to the internal and external environments of the 2D material). Furthermore, a material with a high (low) DOS would then be able to detect smaller (larger) analyte charges.

Above, we also assume uniform and noninterrupted sheets of 2D materials. If the sheet was instead constituted of nanoscopic units arranged in a mesoscale architecture (98), then the potential difference contributing to the capacitance would be mostly concentrated on the surfaces of the units (107) and yield a chemical capacitance: $C_{\text{chem}} = \frac{e.\partial N^i}{(\partial \mu_i/e)}$ (16). In this case, the consideration of the nanostructured entities is done through the change of the number of charge states: N_i (for the ith nanoparticle or grain), corresponding to both the free electrons (of concentration n_c) and the localized or trapped electrons (of concentration n_T for a given change in the chemical potential, μ_i). From the thermodynamic expression (56), we have $\mu_i = \mu_i{}^o + k_B T \ln(N_i)$ and $C_{\text{chem}} = e^2 N_i / k_B T$.

In addition to the capacitances, there would also be resistances associated with the (*a*) electrolyte solution (R_s) between the points of application of voltage and current measurement; (*b*) electron affinity–related potential difference between the electrolyte and the 2D material, i.e., the charge transfer resistance (R_{ct}) (109); and (*c*) finite resistivity of the electrolyte, which yields a shunting resistance (R_{sh}). The diffuse charge layers are represented by a Warburg impedance: Z_W (18). A summary model of the capacitances and resistances is shown in **Figure 3**.

An interesting example of the use of QM-related attributes is the use of a graphene varactor (i.e., a variable capacitor) harnessing the C_Q (**Figure 4**). The C_Q could be of the order of 100 aF/μm and larger than the electrostatic capacitance (20, 50). The coupling to an inductor—either extrinsic or intrinsic to the graphene—yields a characteristic resonance frequency $f_{\text{res}} = \frac{1}{2\pi\sqrt{LC}}$ and would make possible remote interrogation of the sensing through nanocarbon-based THz circuitry (37). While extrinsic electromagnetic inductance would be of the order of 1 pH/μm, exploiting the intrinsic quantum or kinetic inductance, which may be three orders of magnitude larger at nH/μm in graphene (80) or other 2D materials (23), could enable monitoring at the radio frequency (RF) scale.

Glucose detection through monitoring the C_Q on the basis of glucose binding to PBA on the graphene surface has been accomplished (148). The PBA dissociation constant, pK_a (86), is shifted due to the covalent binding of glucose, leading to graphene doping and a consequent modulation

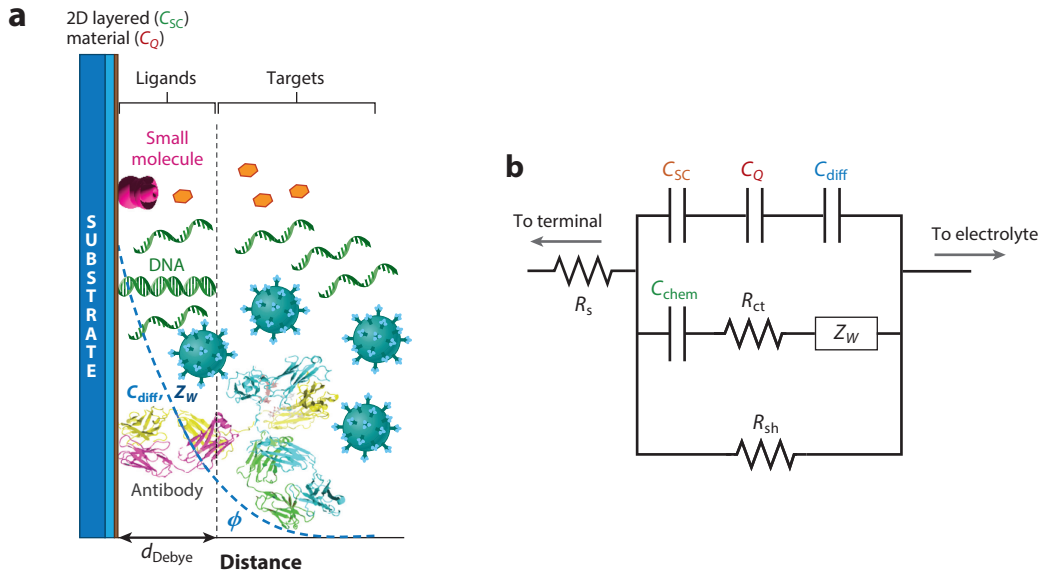

Figure 3

The charge modulations at or near a 2D material surface, through the variation of the electrical potential (ϕ). (*a*) A schematic of the interactions of various biomolecules, ranging from trace elements or small molecules, to DNA, to larger-scale antibody and protein moieties (not to scale), based on data from Reference 61. (*b*) A summary model of the plausible resistance and capacitance elements that must be considered for evaluating biosensor response. The diffusion capacitance (C_{diff}) arises from the electrostatic interactions of the 2D material with the ambient, e.g., electrolyte and biomolecules. The series addition of quantum capacitance (C_Q), which is due to finite density of states and relevant to the lower dimensionality; a space-charge capacitance (C_{SC}) for layered 2D materials such as few-layer graphenes, which is due to the spread of the charge in the structure; and a chemical capacitance or pseudocapacitance (C_{chem}), which is due to localized carrier density on the surface, must all be considered. Additionally, resistance contributions from the solution (R_s), the charge transfer resistance (R_{ct}), and a shunting resistance (R_{sh}), combined with the frequency-dependent impedance of the diffuse charge layers, i.e., the Warburg impedance, Z_W, are relevant.

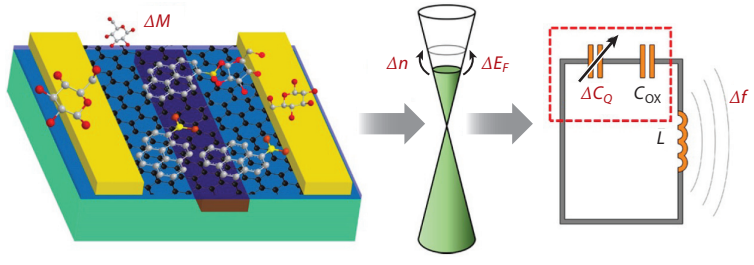

Figure 4

The sensing of an analyte of concentration ΔM on 1-pyrenebutyric acid (PBA) (see **Figure 2**). The surface-functionalized graphene (*left*) would modulate the charge density by Δn and result in a change of the Fermi energy by ΔE_F (*middle*). The Δn changes the quantum capacitance (ΔC_Q), which manifests as a variable capacitor (varactor) in series with a fixed or oxide capacitance (C_{ox}). The integration of the varactor with an inductor (L) constitutes a LC element corresponding to a tunable resonance frequency (Δf). Figure adapted with permission from Reference 148; copyright 2017 American Chemical Society.

of the C_Q. A particularly attractive attribute of 2D materials is thus that they enable the exploitation of QM-related quantum capacitances and inductances.

3.2. Field Effect Transistor–Based Devices for Sensitive Biomolecule Detection

Device modalities and related principles of biological and chemical sensors, based on the use of a FET (90), have been extensively studied over the past five decades, as indicated by the many reviews on the topic (e.g., 24, 61, 88, 112, 117, 133). We outline the basic principles in this section. The version that has been most deployed for biomolecule detection is the ion-sensitive FET (ISFET) version (15). It has been indicated that the ISFET is electronically identical to a metal oxide semiconductor FET (MOSFET) except that it has the additional feature that the interfacial potential at the electrolyte or material interface modulates the threshold voltage (**Figure 5**).

One mode of operation of the FET relevant to biosensing is as follows: An electrical current (I_{ds}) is passed between two electrical contacts on the sensing material, i.e., from the source to the drain, in response to an applied voltage, e.g., V_{ds}. The I_{ds} may be modulated by a gate voltage (V_{gate}), e.g., decreased (increased) by a negative (positive) V_{gate}. The extent of modulation, in terms of magnitude as well as of the polarity, would be a function of the specific moiety on the surface and may be used for the related identification. A typical use of the FET is to transduce surface perturbations from biomolecules into an electrical signal, as illustrated in **Figure 5**, through the layout and the observed signal, i.e., the electrical current, as a function of the V_{gate}. Confounding issues related to the sensitivity to the nonanalyte ambient and the need for both intrinsic and extrinsic calibration are also indicated.

The sensitivity of the ISFET mainly arises from the electrostatic potential variations proximal to the surface, which can be understood through (*a*) the intrinsic buffer capacity and (*b*) the differential capacitance (129). The sensitivity of the FET is unparalleled, e.g., it can detect charge variations at the sub-electron level, may be used to detect subtle variations in biological molecule conformations and interactions, and is an ideal basis for biomedical diagnostics. Another attractive advantage is that FET-based detection may be independent of the necessity of specific chemical reagents, as the detection is based on charge modulation. Consequently, FET-based sensing has been widely used, as is illustrated next.

3.3. Applications in Biomolecule Sensing

As indicated above, the all-surface characteristic of graphene implies extreme sensitivity to even stray and spurious charges. Consequently, both sensitive and specific detection are necessary and need to be quantified. The sensitivity should ideally be parameterized through the (*a*) limit of blank (LoB), the apparent amount of analyte seemingly detected when using a blank sample in the absence of the analyte; (*b*) limit of detection (LoD), the lowest analyte concentration that is reliably and distinctly different than the LoB; and (*c*) limit of quantitation (LoQ) (1), which is equal to or larger than the LoD, given a set specification.

Given the 2D attribute of graphene and the electrostatic influence of biomolecule-related electrical charges and currents from the third dimension, there would naturally be limitations to biomolecule sensing. The d_{Debye} has been indicated as a limitation (66, 122), e.g., in aqueous media, given that $\sim d_{Debye}(nm) \sim \frac{10}{\sqrt{\text{Conc.}(mM)}}$; indeed, with typical extracellular or intracellular fluid concentrations at the order of 100 mM, it would seem that only analytes <1 nm in extent could be monitored. However, such a limitation is not borne out experimentally, where charge modulation at a distance more than 30 times the d_{Debye} was detected (99). An additional Donnan length scale (87), associated with a bulk potential (ϕ_b), and space charge regions, away from the substrate, have been invoked to rationalize the detection of biomolecules beyond d_{Debye}.

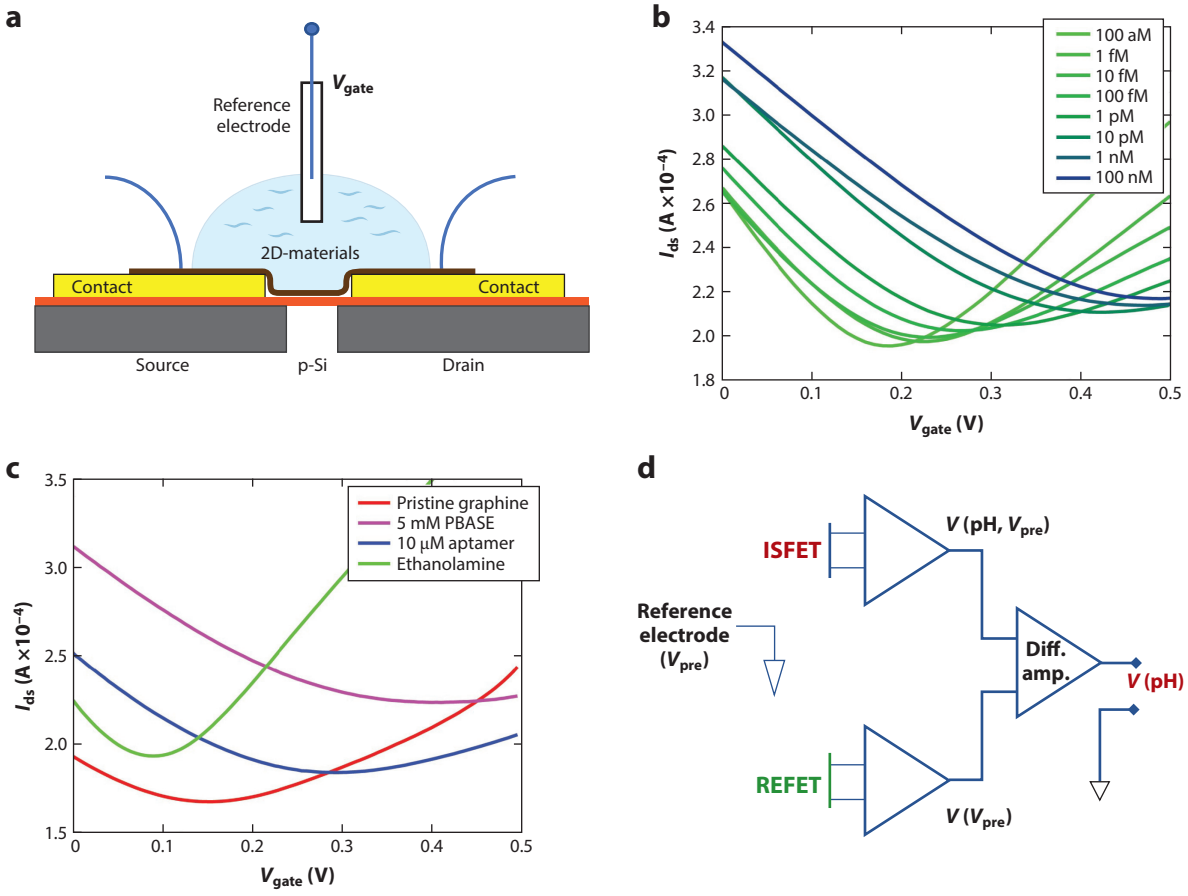

Figure 5

(*a*) An ion-sensitive field effect transistor (ISFET)-based configuration is often deployed for biomolecule detection (15). Subsequent to contact fabrication on Si substrates, a 2D material such as graphene is placed. (*b*) The current between the source and the drain (I_{ds}) with respect to the analyte concentration is modulated as a function of the voltage applied on a gate or reference electrode (V_{gate}). For graphene, the minimum of the I_{ds} (V_{gate}) is termed the Dirac voltage (V_{Dirac}). (*c*) As the changes in the I_{ds} are mainly attributed to the electrostatic potential (129) near the surface, the V_{Dirac} is exquisitely sensitive to the ambient, i.e., the changes on addition of functionalizing agents such as PBASE or capping agents such as ethanolamine, preceding the analyte, e.g., aptamer, addition. (*d*) The robustness of detection may be enhanced using a reference FET (REFET), which is immune to the ambient modulations. The difference between the response of the analyte-sensitive ISFET, shown to be a function of the pH, with respect to the REFET (both monitored with respect to a given reference electrode potential, V_{pre}) is considered through a differential amplifier (Diff. amp.) and yields greater fidelity of detection. Panel *d* adapted with permission from Reference 15.

Below, we discuss some of the instances where 2D materials–based sensing has been deployed. It may seem apparent that sensing should be verified first for the smaller varieties of elements and molecules and then extended to the bigger ensembles. The trace metals, such as As, Cu, Fe, Hg, Pb, and Zn, and minerals in biological media play significant roles in disease detection and nutrigenomic therapies (17). Their detection at the parts per million (ppm) level has been traditionally accomplished in serum and blood, e.g., through mass spectrometry, with LoB and LoD at the μg/L level (70), yielding limits in the μM to nM range. Graphene FET–based techniques may complement extant methods (58) incorporating liquid chromatography–mass

spectroscopy, gas chromatography, enzyme-linked immunosorbent assay, western/northern blot tests, and inductively coupled plasma-based mass spectroscopy (19).

The use of 2D materials–based devices offers portable diagnostics of trace elements, possibly with several orders of magnitude greater sensitivity at the pico- to attomolar (pM–aM) levels (63, 131) compared to biosensors, which deploy non-2D materials. The specificity of sensing, in complex solutions, can be substantially increased by conjugation of an element- or molecule-specific receptor, such as an aptamer (a short, single-stranded DNA or RNA sequence specific to the element or molecule), onto the 2D material. Issues related to sensitivity in a high-salt solution may be addressed by developing dynamic receptor molecules, which cause depletion or enrichment of the charge molecule of interest near the sensor surface (93). An advantage of using such aptamer-like intermediaries is the large possible variety of designs enabling aptasensor-based technologies (115, 132) involving both electrochemical and colorimetry-based schemes (146). For instance, greater specificity in the detection of Pb^{2+} (76, 141, 143), coupled with selectivity over other metal cations (135), has been achieved using FET-based devices. One detection mechanism involves the charge transfer from a molecule, e.g., methylene blue (143), placed at one end of the aptamer, the other end of which is attached to the graphene, and subsequent monitoring of the change in the aptamer conformation due to the interaction of the metal ions. LoDs of the order of ng/L (approximately pM level)—three orders of magnitude lower than the safe blood level of 100 μg/L (135)—for Pb^{2+} and approximately 10 nM for Cu^{2+} (136) were reported through such aptamer-based strategies. Aptamer-based methodologies have also been used to detect multiple analytes, e.g., of different metabolites relevant to opioids, at the picogram/ml level (67).

Detecting larger molecules such as nucleic acids or proteins presents more challenges with respect to sensing fidelity due to the bigger size as well as complex structure conformations. In addition to the charge attribute, properties such as aromaticity and extent of the hydrophobic character of the constituents play significant roles through subsidiary interaction with the substrate (103). A record sensitivity, e.g., at zeptomolar (zM) levels, was achieved for microRNAs (miRNAs) in buffer and biological serum using crumpled graphene-based FET (53). In this case, the 600 zM level of detection implies approximately 18 nucleic acid molecules. The reduced charge screening due to the development of electrical hot spots was implicated in the extremely high-sensitivity values. miRNAs and RNAs are relevant biomarkers for various cancers, neurodegenerative diseases, and viral infections (139). Early detection of such biomarkers can help reduce the risk of disease; thus, their sensitive detection is imperative (125). Poly-L-lysine (PLL)-functionalized graphene FETs were able to detect miRNA and SARS-CoV-2 RNA at the fM range of concentrations within 20 min by utilizing complementary DNA probes specific to the RNA (40). However, DNA probe–based sensors face challenges from a slow hybridization rate, poor specificity, and background noise, and alternative peptide nucleic acid–based probes with higher affinity and lower surface charge may be used for detection at the 100 zM RNA concentration levels (125).

However, the direct determination of specific base position and type of modification in RNA or DNA is still unclear due to nonspecific surface receptor–target interactions. A related innovation in this area involves detecting synthetic nucleic acid sequences of well-defined length (6, 55, 104) at nM to aM levels (21). An ability to discriminate at the single-mutation level, as would be relevant to various neurological disorders and cardiovascular diseases (6), is the goal. Watson-Crick hybridization–mediated differences caused by base modification and single-nucleotide polymorphisms (SNPs) (54, 101) cause an electrical current modulation on the 2D material surface. The sensitivity to SNPs may be further improved by conjugation of partially double-stranded probes close to the surface and reconfiguration of toe-hold regions in the middle of the probe (55). Such a probe configuration was used for label-free detection of site-specific cytosine methylation in synthetic nucleotide fragments related to glioblastoma (6). The plausible nucleic acid

base–2D material surface interaction confounds clear discrimination when multiple mutations are involved. Recent efforts to mitigate such issues involve analyzing genome engineering related to CRISPR/Cas-based DNA interaction (5) through FET architecture. As an example, SARS-CoV-2- and respiratory syncytial virus–based genes were detected using graphene FETs without amplification of RNA at the LoD of 1 aM (74).

An alternate scheme for genome-related sequencing (138) involves the creation and use of a nanopore (35, 144) of a specific length scale (of the order of 2 nm) incorporated into 2D material–based FETs (41, 44). Initially, structure-specific interference of ionic conductivity across the nanopore was utilized for the spatial discrimination of the genome constituents (89, 113). However, reliably fabricating nanopores and overcoming low sensitivity and high speed of translocation, which yield a reduced signal-to-noise ratio (138), are challenges. Recent advances in detecting transverse currents, for instance, across 2D MoS_2 membranes, due to direct interaction of DNA bases may provide better temporal resolution compared to traditional methods that measure ionic current along the pore (44). Indeed, such compound 2D materials, in contrast to the relatively inert graphene, have a propensity for enhanced electrocatalytic reactions and high current density, enabling sensitivity superior to extant bulk electrochemical sensors.

Confounding factors related to sensing must also be carefully considered. For instance, most studies have been carried out in rather controlled conditions within well-characterized ambients, which may not always be practically relevant. Moreover, passive detection of larger biomolecules such as proteins should also be subject to further inquiry. For instance, it has been indicated that the greater extent of planarity in 2D materials may induce substantial conformational changes into the structural elements of proteins such as α-helices and β-sheets (4). Such issues provide motivation for the development of alternate schemes.

3.4. Alternate Modalities for Sensing

Sensors exploiting the principles of surface plasmon resonance (SPR) provide an alternate mode of biomolecule analysis exploiting the surface-specific attributes of 2D materials. The basis of SPR is the modulation of electromagnetic surface waves, termed surface plasmons (108), that arise at the interface of a positive-ε and a negative-ε medium. The in-plane dielectric constant ($\varepsilon_{||}$) of graphene may be made negative by varying the carrier density in the near-infrared regime and helps support a graphene surface plasmon polariton (GrSPP). The related surface plasmon polariton (SPP) resonance peak would be sensitive to an analyte or moiety as transduced through the peak shift (in wavelength units) with respect to a given refractive index ($\tilde{n}$) change in units of nm/refractive index unit (RIU). With the analyte adsorbed on the graphene surface, variation of the $\tilde{n}_{\text{analyte}}$ from approximately 1.3 (e.g., for glucose) to 1.7 (e.g., for mutagens such as diiodomethane) could be indicated through a shift of the SPP resonances. The GrSPP-related peaks show a sensitivity of approximately 150 nm/RIU (33) as monitored at the 800 nm wavelength, which, given a nominal spectrometer resolution of 0.1 nm, implies that a refractive index (dielectric constant) difference of the order of 10^{-3} (10^{-6}) due to the adsorbing moiety may be detected.

4. OUTLOOK FOR FUTURE DEVELOPMENTS

An obviously attractive aspect of the use of 2D structures for biomolecule sensing is related to the relatively increased surface sensing area and the smaller amount of material needed, motivating the use of miniaturized devices in line with modern technological development. In terms of sensitivity, 2D materials are unique; for example, one-dimensional (1D) nanowire–based sensors have been indicated to yield high sensitivity only at particular points of contact due to curvature effects (118),

while zero-dimensional (0D) quantum dots suffer from issues related to their size variation, poor interfaces, and consequent weak electrical coupling (47).

Such considerations have propelled 2D materials to the forefront of biosensing. However, the impetus to make things smaller may not provide enough motivation for development given the issues with specificity. What could generate more enthusiasm for a concerted effort to apply 2D materials widely as sensors is the harnessing of additional scientific principles. A few instances of the use of QM principles related to quantum capacitance and quantum or kinetic inductance, and their subsequent transduction to THz or RF-based interrogation of the diagnostics, have been previously discussed (111). Moreover, lower dimensionality leads to energy quantization, which may be utilized for moiety-specific detection. It would thus be relevant to delve into such principles in the service of molecule sensing. Additionally, intrinsic as well as extant issues with the standardization of the material and testing protocols must be clearly delineated, as is discussed next.

4.1. Defects and Nonuniformity of 2D Film Morphology: Need for Standardization Protocols, Reliability, and Comparison of Measurements

The Mermin-Wagner theorem (48, 62) has often been cited with reference to the impossibility of long-range crystalline order in 2D systems at finite temperatures. The implication, with respect to biosensing, would be the existence of intrinsic out-of-plane corrugations and ripples, of the order of 0.1 nm or much larger, on the surface (62). Moreover, considering the impossibility of a defect-free material, in the entropic sense, one must contend with a rippled and defective material in a practical or experimental graphene flake of finite size that is deployed in a sensor. There is then an imperative to (*a*) acknowledge the types of defects that may be present (11) and (*b*) determine possible ways to eliminate or engineer such defects. For instance, specific defects in a graphene sheet with (without) localized electron density, i.e., the zigzag (armchair)-related single-atom vacancies, could be created through conventional plasma processing (94). The zigzag variety could contribute to an enhanced DOS (92) and selectively modulate the C_Q. Furthermore, the single-atom vacancy constitutes the smallest possible nanopore.

Considering such defects, and the inevitability of defective material particular to the use of nanostructures (11, 49, 94), emphasizes the need to adopt a standardized material, e.g., per a set list of calibrations over a series of steps, as indicated in **Figure 5*c***. This may be accomplished, for instance, in graphene through monitoring the initial V_D (**Figure 5*b***) and ensuring that the films selected for further device processing are within a select range of the chosen metric.

Indeed, statistical methodologies should also be adopted more widely in the community with respect to the rigor of the measurements; this would provide information on the reliability of the testing, especially when impure or mixed samples are being analyzed. For instance, the biosensing modality should guard against both false positives (Type I errors) and false negatives (Type II errors) (134). A sensing test with low rates of false positives (negatives) would be expected to have high specificity (sensitivity). The roadmap perspective adopted by the semiconductor industry could be a guiding light "to improve the links between academia and industry, to stimulate investments, to provide elements for future research programs and activities, and to coordinate efforts to propose the most promising solutions" (42, p. 308). Subsequent forays into new technologies may encourage the development of novel biosensing science.

4.2. Harnessing Quantum Mechanics in Sensing: Molecular and Energy-Related Specificity

Switching to a QM point of view also brings to the forefront energy scales, in contrast to the mostly Newtonian force–based descriptions that are in vogue for 2D materials–based sensors.

Such a point of view could consider lower-dimensional structures, such as 1D nanowires (128) or 0D quantum dots (3, 126), which may be present in islands of interrupted graphene or may be constituted from graphene itself. Moreover, a structure with decreased dimensionality, imbedded in the 2D material, also enhances the DOS at a lower energy (10, 95). The implication is that 2D materials–based sensors may provide greater sensitivity at a lower applied voltage.

Consequently, the energy scales specific to a particular biomolecule moiety may be tuned and harnessed. The fact that the energy levels are discrete and finite may enable correspondent molecular-level sensing; for example, a moiety conformation with an energy of approximately 10 meV may perhaps be discriminated from another. However, the coupling of the energy levels to the environment could induce a nonunique spread to the levels, e.g., through electrical contacts, and must be considered as well. The linkage between the nanoscopic moieties in 2D materials would then be relevant for the transduction of the sensing to electrons and a current for viable biosensors. While quantum structures possess energy specificity, the detection of a finite quantity of biomolecules, e.g., of the order of 1 molecule in 1 ml of analyte, at the state-of-the-art zM level (32, 53) still demands repeated measurements.

4.3. Summary

2D materials are unique lower-dimensional systems that provide new paradigms of biomolecule detection. Large surface area coupled with the capability to tune the carrier density harnesses classical and QM attributes. However, as we indicate above, while the sensitivity is superior to any other sensing systems, there are also issues related to extreme responsiveness. Consequently, careful attention must be paid to all possible sources of errors while adhering to quantitative measures and established standards (124). The latter would be important for comparing the studies from different laboratories.

The adoption of 2D materials–based technologies for biosensors, configured for lab-on-a-chip platforms and enabling point-of-care modalities (120), would represent a significant step toward miniaturization of health care diagnostics—moving away from extant methods, such as optical sensing and thermal amplification, which are handicapped by low resolution, slow speeds, and bulky support systems. When materials- and device-related issues are resolved, especially with respect to specificity, 2D materials–based biosensors will enable economical and rapid detection of trace element contamination, disease biomarkers, antibiotics, etc. and truly revolutionize health care around the world.

DISCLOSURE STATEMENT

The authors are not aware of any affiliations, memberships, funding, or financial holdings that might be perceived as affecting the objectivity of this review.

ACKNOWLEDGMENTS

The authors thank A. Lee for assistance in the preparation of **Figure 1**. The authors also acknowledge the research and financial support of the RadX initiative of the National Institutes of Health, the National Science Foundation (NSF), and the Army Research Office. They apologize in advance to colleagues whose work was not cited due to space limitations.

LITERATURE CITED

1. Armbruster DA, Pry T. 2008. Limit of blank, limit of detection and limit of quantitation. *Clin. Biochem. Rev.* 29(Suppl. 1):S49–52

2. Ashcroft NW, Mermin ND. 1976. *Solid State Physics*. Orlando, FL: Saunders Coll.
3. Bacon M, Bradley SB, Nann T. 2013. Graphene quantum dots. *Part. Part. Syst. Charact.* 31(4):415–28
4. Balamurugan K, Subramanian V. 2022. Interaction of amino acids, peptides, and proteins with two-dimensional carbon materials. *Theor. Comput. Chem.* 21:191–210
5. Balderston S, Taulbee JJ, Celaya E, Fung K, Jiao A, et al. 2021. Discrimination of single-point mutations in unamplified genomic DNA via Cas9 immobilized on a graphene field-effect transistor. *Nat. Biomed. Eng.* 5:713–25
6. Ban DK, Liu Y, Wang Z, Ramachandran S, Sarkar N, et al. 2020. Direct DNA methylation profiling with an electric biosensor. *ACS Nano* 14(6):6743–51
7. Bandaru PR. 2007. Electrical properties and applications of carbon nanotube structures. *J. Nanosci. Nanotechnol.* 7:1239–67
8. Bandaru PR, Pichanusakorn P. 2010. An outline of the synthesis and properties of silicon nanowires. *Semicond. Sci. Technol.* 25:024003
9. Bandaru PR, Yamada H, Narayanan R, Hoefer M. 2015. Charge transfer and storage in nanostructures. *Mater. Sci. Eng. R* 96:1–69
10. Bandaru PR, Yamada H, Narayanan R, Hoefer M. 2017. The role of defects and dimensionality in influencing the charge, capacitance, and energy storage of graphene and 2D materials. *Nanotechnol. Rev.* 6(5):421–33
11. Banhart F, Kotakoski J, Krasheninnikov AV. 2011. Structural defects in graphene. *ACS Nano* 5:26–41
12. Banszerus L, Schmitz M, Engels S, Dauber J, Oellers M, et al. 2015. Ultrahigh-mobility graphene devices from chemical vapor deposition on reusable copper. *Sci. Adv.* 1(6):e1500222
13. Barbieri O, Kötz R. 2005. Capacitance limits of high surface area activated carbons for double layer capacitors. *Carbon* 43:1303–10
14. Bard AJ, Faulkner LR. 2001. *Electrochemical Methods: Fundamentals and Applications*. Hoboken, NJ: Wiley
15. Bergveld P. 2003. Thirty years of ISFETOLOGY: what happened in the past 30 years and what may happen in the next 30 years. *Sens. Actuators B* 88:1–20
16. Bisquert J. 2003. Chemical capacitance of nanostructured semiconductors: its origin and significance for nanocomposite solar cells. *Phys. Chem. Chem. Phys.* 5(24):5360–64
17. Braicu C, Mehterov N, Vladimirov B, Sarafian V, Nabavi SM, et al. 2017. Nutrigenomics in cancer: revisiting the effects of natural compounds. *Semin. Cancer Biol.* 46:84–106
18. Brett CMA, Brett AMO. 1993. *Electrochemistry: Principles, Methods, and Applications*. Oxford, UK: Oxford Univ. Press
19. Bulska E, Ruszczyńska A. 2017. Analytical techniques for trace element determination. *Phys. Sci. Rev.* 2(5):20178002
20. Burke PJ. 2002. Luttinger liquid theory as a model of the gigahertz electrical properties of carbon nanotubes. *IEEE Trans. Nanotechnol.* 1:129–44
21. Campos R, Borme J, Guerreiro JR, Machado G, Cerqueria MF, et al. 2019. Attomolar label-free detection of DNA hybridization with electrolyte-gated graphene field-effect transistors. *ACS Sens.* 4:286–93
22. Chae M-S, Yoo YK, Kim J, Kim TG, Hwang KS. 2018. Graphene-based enzyme-modified field-effect transistor biosensor for monitoring drug effects in Alzheimer's disease treatment. *Sens. Actuators B* 272:448–58
23. Chanana A, Loftizadeh N, Quispe HOC, Gopalan P, Winger JR, et al. 2019. Manifestation of kinetic-inductance in spectrally-narrow terahertz plasmon resonances in thin-film Cd3As2. *ACS Nano* 13:4091
24. Chaniotakis N, Fousaki M. 2014. Bio-chem-FETs: field effect transistors for biological sensing. In *Biological Identification: DNA Amplification and Sequencing, Optical Sensing, Lab-on-Chip and Portable Systems*, ed. RP Schaudies, pp. 194–219. Sawston, UK: Woodhead Publ.
25. Chen RJ, Zhang Y, Wang DZ, Dai H. 2001. Noncovalent sidewall functionalization of single-walled carbon nanotubes for protein immobilization. *J. Am. Chem. Soc.* 123:3838–39
26. Chen X, Liu Y, Fang X, Li Z, Pu H, et al. 2019. Ultratrace antibiotic sensing using aptamer/graphene-based field-effect transistors. *Biosens. Bioelectron.* 126:664–71
27. Compton OC, Nguyen ST. 2010. Graphene oxide, highly reduced graphene oxide, and graphene: versatile building blocks for carbon-based materials. *Small* 6:711–23

28. Conway BE, Bockris JO, Ammar IA. 1951. The dielectric constant of the solution in the diffuse and Helmholtz double layers at a charged interface in aqueous solution. *Trans. Faraday Soc.* 47:756–66
29. Datta S. 2005. *Quantum Transport: Atom to Transistor*. Cambridge, UK: Cambridge Univ. Press
30. de Gennes P-G, Brochard-Wyart F, Quere D. 2002. *Capillarity and Wetting Phenomena: Drops, Bubbles, Pearls, Waves*. Berlin: Springer
31. Delahay P. 1965. *Double Layer and Electrode Kinetics*. New York: Interscience
32. Dhanapala L, Jones AL, Czarnecki P, Rusling JF. 2020. Sub-zeptomole detection of biomarker proteins using a microfluidic immunoarray with nanostructured sensors. *Anal. Chem.* 92:8021–25
33. Dong Y, Bandaru PR. 2022. Enhanced graphene surface plasmonics through incorporation into metallic nanostructures. *Opt. Express* 30:30696–704
34. Dontschuk D, Stacey A, Tadich A, Rietwyk KJ, Schenk A, et al. 2015. A graphene field-effect transistor as a molecule-specific probe of DNA nucleobases. *Nat. Commun.* 6:6563
35. Drndić M. 2021. 20 years of solid-state nanopores. *Nat. Rev. Phys.* 3:606
36. Dundas CM, Demonte D, Park S. 2013. Streptavidin-biotin technology: improvements and innovations in chemical and biological applications. *Appl. Microbiol. Biotechnol.* 97:9343–53
37. Faraby HM, Rao AM, Bandaru PR. 2013. Modeling high energy density electrical inductors operating at THz frequencies based on coiled carbon nanotubes. *IEEE Electron. Device Lett.* 34(6):807–9
38. Feynman RP, Leighton RB, Sands M. 1964. *The Feynman Lectures in Physics*. New York: Addison Wesley
39. Firme CP III, Bandaru PR. 2010. Toxicity issues in the application of carbon nanotubes to biological systems. *Nanomed. Nanotechnol. Biol. Med.* 6(2):245–56
40. Gao J, Wang C, Wang C, Chu Y, Wang S, et al. 2022. Poly-L-lysine-modified graphene field-effect transistor biosensors for ultrasensitive breast cancer miRNAs and SARS-CoV-2 RNA detection. *Anal. Chem.* 94:1626–36
41. Garaj S, Hubbard W, Reina A, Kong J, Branton D, Golovchenko JA. 2010. Graphene as a subnanometre trans-electrode membrane. *Nature* 467(7312):190–93
42. Gargini P, Balestra F, Hayashi Y. 2022. Roadmapping of nanoelectronics for the new electronics industry. *Appl. Sci.* 12:308
43. Gerischer H. 1997. Principles of electrochemistry. In *The CRC Handbook of Solid State Electrochemistry*, ed. PJ Gellings, HJM Bouwmeester, pp. 9–74. Boca Raton, FL: CRC Press
44. Graf M, Lihter M, Altus D, Marion S, Radenovic A. 2019. Transverse detection of DNA using a MoS2 nanopore. *Nanoletters* 19(12):9075–83
45. Graham SA, Boyko E, Salama R, Segal E. 2020. Mass transfer limitations of porous silicon-based biosensors for protein detection. *ACS Sens.* 5:3058–69
46. Grahame DC. 1947. The electrical double layer and the theory of electrocapillarity. *Chem. Rev.* 41(3):441–501
47. Guyot-Sionnest P. 2012. Electrical transport in colloidal quantum dot films. *J. Phys. Chem. Lett.* 3:1169–75
48. Halperin BI. 2019. On the Hohenberg-Mermin-Wagner theorem and its limitations. *J. Stat. Phys.* 175:521–29
49. Hoefer MA, Bandaru PR. 2010. Defect engineering of the electrochemical characteristics of carbon nanotube varieties. *J. Appl. Phys.* 108(3):034308
50. Hossain MF, Hassan A, Rana MS. 2014. Theoretical investigation of quantum capacitance in armchair-edge graphene nanoribbons. In *Proceedings of the 2013 International Conference on Electrical Information and Communication Technology (EICT), Khulna, Bangladesh, Feb. 13–15*, art. 14197054. Piscataway, NJ: IEEE
51. Hughes ZE, Walsh TR. 2015. What makes a good graphene-binding peptide? Adsorption of amino acids and peptides at aqueous graphene interfaces. *J. Mater. Chem. B* 3:3211–21
52. Hummers WS, Offemann RE. 1958. Preparation of graphitic oxide. *J. Am. Chem. Soc.* 80:1339
53. Hwang MT, Heiranian M, Kim Y, You S, Leem J, et al. 2020. Ultrasensitive detection of nucleic acids using deformed graphene channel field effect biosensors. *Nat. Commun.* 11(1):1543
54. Hwang MT, Landon PB, Lee J, Choi D, Mo AH, et al. 2016. Highly specific SNP detection using 2D graphene electronics and DNA strand displacement. *PNAS* 113(26):7088–93
55. Hwang MT, Wang Z, Ping J, Ban DK, Shiah ZC, et al. 2018. DNA nanotweezers and graphene transistor enable label-free genotyping. *Adv. Mater.* 30:1802440

56. Ibach H, Luth H. 1991. *Solid-State Physics: An Introduction to Theory and Experiment*. Berlin: Springer
57. Israelachvili JN. 2011. *Intermolecular and Surface Forces*. San Diego: Academic. 3rd ed.
58. Ivanenko NB, Ganeev AA, Solovyev ND, Moskvin LN. 2011. Determination of trace elements in biological fluids. *J. Anal. Chem.* 66(9):784
59. Jarmoskaite I, AlSadhan I, Vaidyanathan PP, Herschlag D. 2020. How to measure and evaluate binding affinities. *eLife* 9:e57264
60. Kagan VE, Bayir H, Shvedova AA. 2005. Nanomedicine and nanotoxicology: two sides of the same coin. *Biol. Med.* 4:313–16
61. Kaisti M. 2017. Detection principles of biological and chemical FET sensors. *Biosens. Bioelectron.* 98:437–48
62. Katsnelson MI. 2012. *Graphene: Carbon in Two Dimensions*. Cambridge, UK: Cambridge Univ. Press
63. Khomyakov PA, Giovannetti G, Rusu PC, Brocks G, van den Brink J, Kelly PJ. 2009. First-principles study of the interaction and charge transfer between graphene and metals. *Phys. Rev. B* 79(19):195425
64. Kim J, Park S-J, Min D-H. 2017. Emerging approaches for graphene oxide biosensor. *Anal. Chem.* 89(1):232–48
65. Kopp T, Mannhart J. 2009. Calculation of the capacitances of conductors: perspectives for the optimization of electronic devices. *J. Appl. Phys.* 106:064504
66. Kulkarni GS, Zhong Z. 2012. Detection beyond the Debye screening length in a high-frequency nanoelectronic biosensor. *Nano Lett.* 12(2):719–23
67. Kumar N, Rana M, Geiwitz M, Khan NI, Catalano M, et al. 2022. Rapid, multianalyte detection of opioid metabolites in wastewater. *ACS Nano* 16:3704–14
68. Kuroda MA, Tersoff J, Martyna GJ. 2011. Nonlinear screening in multilayer graphene systems. *Phys. Rev. Lett.* 106(11):116804
69. Kyte J, Doolittle RF. 1982. A simple method for displaying the hydropathic character of a protein. *J. Mol. Biol.* 157:105–32
70. Laur N, Kinscherf R, Pomytkin K, Kaiser L, Knes O, Deigner H-P. 2020. ICP-MS trace element analysis in serum and whole blood. *PLOS ONE* 15:e0233357
71. Lee J, Kim J, Kim S, Min D-H. 2016. Biosensors based on graphene oxide and its biomedical application. *Adv. Drug Deliv. Rev.* 105:275–87
72. Lewerenz HJ. 2013. On the structure of the Helmholtz layer and its implications on electrode kinetics. *ECS Trans.* 50:3–20
73. Li D, Zhang W, Yu X, Wang Z, Su Z, Wei G. 2016. When biomolecules meet graphene: from molecular level interactions to material design and applications. *Nanoscale* 8:19491–509
74. Li H, Yang J, Wu G, Weng Z, Song Y, et al. 2022. Amplification-free detection of SARS-CoV-2 and respiratory syncytial virus using CRISPR Cas13a and graphene field-effect transistors. *Angew. Chem.* 61:e202203826
75. Li Q, Song J, Besenbacher F, Dong M. 2015. Two-dimensional material confined water. *Acc. Chem. Res.* 48(1):119–27
76. Li Y, Wang C, Zhu Y, Zhou X, Xiang Y, et al. 2017. Fully integrated graphene electronic biosensor for label-free detection of lead (II) ion based on G-quadruplex structure-switching. *Biosens. Bioelectron.* 89:758–63
77. Lin K, Xie L, Tian Y, Liu D. 2016. Au-modified monolayer MoS2 sensor for DNA detection. *J. Phys. Chem. C* 120:11204–9
78. Liu B, Pappas CG, Ottelé J, Schaeffer G, Jurissek C, et al. 2020. Spontaneous emergence of self-replicating molecules containing nucleobases and amino acids. *J. Am. Chem. Soc.* 142:4184–92
79. Liu D, Lipponen K, Quan P, Wan X, Zhang H, et al. 2018. Impact of pore size and surface chemistry of porous silicon particles and structure of phospholipids on their interactions. *ACS Biomater. Sci. Eng.* 4:2308–13
80. Liu Y. 2016. *Modeling of Transport Phenomena in Two-Dimensional Semiconductors*. Minneapolis: Univ. Minnesota
81. Liu Z, Jiang L, Galli F, Nederlof I, Olsthoorn RC, et al. 2010. A graphene oxide˙streptavidin complex for biorecognition—towards affinity purification. *Adv. Funct. Mater.* 20:2857–65

82. Lu C, Liu Y, Ying Y, Liu J. 2017. Comparison of MoS2, WS2, and graphene oxide for DNA adsorption and sensing. *Langmuir* 33:630–37
83. Lu C-H, Yang H-H, Zhi C-L, Chen X, Chen G-N. 2009. A graphene platform for sensing biomolecules. *Angew. Chem.* 48:4785–87
84. Lu H-W, Kane AA, Parkinson J, Gao Y, Hajian R, et al. 2022. The promise of graphene-based transistors for democratizing multiomics studies. *Biosens. Bioelectron.* 195:113605
85. Marcano DC, Kosynkin DV, Berlin JM, Sinitskii A, Sun Z, et al. 2010. Improved synthesis of graphene oxide. *ACS Nano* 4(8):4806–14
86. Marcus RA. 1968. Theoretical relations among rate constants, barriers, and Broensted slopes of chemical reactions. *J. Phys. Chem.* 72(3):891–99
87. Mauro A. 1962. Space charge regions in fixed charge membranes and the associated property of capacitance. *Biophys. J.* 2:179–98
88. Meng Z, Stolz RM, Mendeckki L, Mirica KA. 2019. Electrically-transduced chemical sensors based on two-dimensional nanomaterials. *Chem. Rev.* 119:478–598
89. Merchant CA, Healy K, Wanunu M, Ray V, Pterman N, et al. 2010. NA translocation through graphene nanopores. *Nanoletters* 10:2915–21
90. Muller RS, Kamins TI. 1986. *Device Electronics for Integrated Circuits*. New York: Wiley. 2nd ed.
91. Munief W-M, Lu X, Teucke T, Wilhelm J, Britz A, et al. 2019. Reduced graphene oxide biosensor platform for the detection of NT-proBNP biomarker in its clinical range. *Biosens. Bioelectron.* 126:136–42
92. Nakada K, Fujita M, Dresselhaus G, Dresselhaus M. 1996. Edge state in graphene ribbons: nanometer size effect and edge shape dependence. *Phys. Rev. B* 54(24):17954–61
93. Nakatsuka N, Yang KA, Abendroth JM, Cheung KM, Xu X, et al. 2018. Aptamer-field-effect transistors overcome Debye length limitations for small-molecule sensing. *Science* 362:319–24
94. Narayanan R, Yamada H, Karakaya M, Podila R, Rao AM, Bandaru PR. 2015. Modulation of the electrostatic and quantum capacitances of few layered graphenes through plasma processing. *Nano Lett.* 15(5):3067–72
95. Narayanan R, Yamada H, Marin BC, Zaretski A, Bandaru PR. 2017. Dimensionality-dependent electrochemical kinetics at the single-layer graphene-electrolyte interface. *J. Phys. Chem. Lett.* 8(17):4004–8
96. Nelson DL, Cox MM. 2012. *Lehninger Principles of Biochemistry*. New York: W.H. Freeman Co. 6th ed.
97. Ni C, Chattopadhyay J, Billups WE, Bandaru PR. 2008. Modification of the electrical characteristics of single wall carbon nanotubes through selective functionalization. *Appl. Phys. Lett.* 93(24):243113
98. O'Regan B, Grätzel M. 1991. A low-cost, high-efficiency solar cell based on dye-sensitized colloidal TiO_2 films. *Nature* 353(6346):737–40
99. Palazzo G, De Tullio D, Magliulo M, Mallardi A, Intranuovo F, et al. 2015. Detection beyond Debye's length with an electrolyte-gated organic field-effect transistor. *Adv. Mater.* 27:911–16
100. Panigrahi S, Bhattacharya A, Banerjee S, Bhattacharya D. 2012. Interaction of nucleobases with wrinkled graphene surface: dispersion corrected DFT and AFM studies. *J. Phys. Chem. C* 116:4374–79
101. Pei H, Lu N, Wen Y, Song S, Liu Y, et al. 2010. A DNA nanostructure-based biomolecular probe carrier platform for electrochemical biosensing. *Adv. Mater.* 22(42):4754–58
102. Peigney A, Laurent C, Flahaut E, Basca RR, Rousset A. 2001. Specific surface area of carbon nanotubes and bundles of carbon nanotubes. *Carbon* 39:507–14
103. Pérez E, Martín N. 2015. π-π interactions in carbon nanostructures. *Chem. Soc. Rev.* 44:6425–33
104. Ping J, Vishnubhotla R, Vrudhula A, Johnson ATC. 2016. Scalable production of high-sensitivity, label-free DNA biosensors based on back-gated graphene field effect transistors. *ACS Nano* 10:8700–4
105. Pop E, Varshney V, Roy AK. Thermal properties of graphene: fundamentals and applications. *MRS Bull.* 37:1273–81
106. Pu F, Ren J, Qu X. 2017. Nucleobases, nucleosides, and nucleotides: versatile biomolecules for generating functional nanomaterials. *Chem. Soc. Rev.* 47:1285–306
107. Radovic LR. 2010. Surface chemical and electrochemical properties of carbons. In *Carbons for Electrochemical Energy Storage and Conversion Systems*, ed. F Beguin, E Frackowiak, pp. 163–220. Boca Raton, FL: CRC Press
108. Raether H. 1988. *Surface Plasmons*. Berlin: Springer

109. Rieger PH. 1994. *Electrochemistry*. London: Chapman & Hall. 2nd ed.
110. Roth E, Azaria AG, Girshevitz O, Bitler A, Garini Y. 2018. Measuring the conformation and persistence length of single-stranded DNA using a DNA origami structure. *Nanoletters* 18:6703–9
111. Rutherglen C, Burke P. 2009. Nanoelectromagnetics: circuit and electromagnetic properties of carbon nanotubes. *Small* 5:884–96
112. Sakata T. 2019. Biologically coupled gate field-effect transistors meet in vitro diagnostics. *ACS Omega* 4:11852–62
113. Schneider GF, Kowalczyk SW, Calado VE, Pandraud G, Zandbergen HW, et al. 2010. DNA translocation through graphene nanopores. *Nanoletters* 10:3163–67
114. Seabra AB, Paula AJ, de Lima R, Alves OL, Durán N. 2014. Nanotoxicity of graphene and graphene oxide. *Chem. Res. Toxicol.* 27:159–68
115. Shaban SM, Kim D-H. 2021. Recent advances in aptamer sensors. *Sensors* 21:979
116. Shi H. 1996. Activated carbons and double layer capacitance. *Electrochim. Acta* 41(10):1633–39
117. Shoorideh K. 2016. *Understanding and optimization of field-effect transistor-based biological and chemical sensors*. PhD Diss., Univ. Calif., Los Angeles
118. Shoorideh K, Chui CO. 2014. On the origin of enhanced sensitivity in nanoscale FET-based biosensors. *PNAS* 111:5111–16
119. So CR, Hayamizu Y, Yazici H, Gresswell C, Khatayevich D, et al. 2012. Controlling self-assembly of engineered peptides on graphite by rational mutation. *Nanoletters* 6:1648–56
120. Song Y, Huang Y-Y, Lu X, Zhang X, Ferrari M, Qin L. 2014. Point-of-care technologies for molecular diagnostics using a drop of blood. *Trends Biotechnol.* 32(3):132–39
121. Su TA, Neupane M, Steigerwald ML, Venkataraman L, Nuckolls C. 2016. Chemical principles of single-molecule electronics. *Nat. Rev. Mater.* 1:16002
122. Swaminathan VV, Dak P, Reddy B, Salm E, Duarte-Guevara C, et al. 2015. Electronic desalting for controlling the ionic environment in droplet-based biosensing platforms. *Appl. Phys. Lett.* 106(5):300–78
123. Sze SM. 2003. *Semiconductor Devices: Physics and Technology*. New York: Wiley. 2nd ed.
124. Tholen DW, Linnet K, Kondratovich M, Armbruster DA, Garrett PE, et al. 2004. *Protocols for determination of limits of detection and limits of quantitation; approved guideline*. NCCLS Doc. EP17-A, Natl. Comm. Clin. Lab. Stand., Wayne, PA. **https://webstore.ansi.org/preview-pages/CLSI/preview_EP17-A.pdf**
125. Tian M, Qiao M, Shen C, Meng F, Frank LA, et al. 2020. Highly-sensitive graphene field effect transistor biosensor using PNA and DNA probes for RNA detection. *Appl. Surf. Sci.* 527:146839
126. Tian P, Tang L, Teng KS, Lau SP. 2018. Graphene quantum dots from chemistry to applications. *Mater. Today* 10:221–58
127. Tkachev SV, Buslaeva RY, Naumkin AV, Kotova SL, Laure IV, Gubin SP. 2012. Reduced graphene oxide. *Inorg. Mater.* 48(8):796–802
128. Vadlamani SK. 2021. *Sharp switching in tunnel transistors and physics-based machines for optimization*. PhD Diss., Univ. Calif., Berkeley
129. van Hal REG, Eijkel JCT, Bergveld P. 1995. A novel description of ISFET sensitivity with the buffer capacity and double layer capacitance as key parameters. *Sens. Actuators B* 24:201–5
130. Varghese N, Mogera U, Govindaraj A, Das A, Maiti PK, et al. 2009. Binding of DNA nucleobases and nucleosides with graphene. *Chem. Phys. Chem.* 10:206–10
131. Varghese SS, Lonkar S, Singh K, Swaminathan S, Abdala A. 2015. Recent advances in graphene based gas sensors. *Sens. Actuators B* 218:160–83
132. Vishnubhotla R, Ping J, Gao Z, Lee A, Saouaf O, et al. 2017. Scalable graphene aptasensors for drug quantification. *AIP Adv.* 7:115111
133. Vu C-A, Chen W-Y. 2019. Field-effect transistor biosensors for biomedical applications: recent advances and future prospects. *Sensors* 19:4214
134. Walpole RE, Myers RH, Myers SL. 1998. *Probability and Statistics for Engineers and Scientists*. Upper Saddle River, NJ: Prentice-Hall Inc. 6th ed.
135. Wang C, Cui X, Li Y, Li H, Haung L, et al. 2016. A label-free and portable graphene FET aptasensor for children blood lead detection. *Sci. Rep.* 6:21711
136. Wang R, Cao Y, Qu H, Wang Y, Zheng L. 2022. Label-free detection of Cu(II) in fish using a graphene field-effect transistor gated by structure-switching aptamer probes. *Talanta* 237:122965

137. Wang Y, Chen Y, Lacey SD, Xu L, Xie H, et al. 2018. Reduced graphene oxide film with record-high conductivity and mobility. *Mater. Today* 21:186–92
138. Wasfi A, Awwad F, Ayesh AI. 2018. Graphene-based nanopore approaches for DNA sequencing: a literature review. *Biosens. Bioelectron.* 119:191–203
139. Watson JD, Baker TA, Bell SP, Gann A, Levine M, Losick R. 2013. *Molecular Biology of the Gene*. London: Pearson. 7th ed.
140. Webb TJ. 1926. The free energy of hydration of ions and the electrostriction of the solvent. *J. Am. Chem. Soc.* 48(10):2589–603
141. Wen Y, Li FY, Dong X, Zhang J, Xiong Q, Chen P. 2013. The electrical detection of lead ions using gold-nanoparticle- and DNAzyme-functionalized graphene device. *Adv. Healthc. Mater.* 2:271–74
142. Xu H, Zhu J, Ma Q, Ma J, Bai H, et al. 2021. Two-dimensional MoS2: structural properties, synthesis methods, and regulation strategies toward oxygen reduction. *Micromachines* 12:240
143. Xu K, Meshik X, Nichols BM, Zakar E, Dutta M, Stroscio MA. 2014. Graphene- and aptamer-based electrochemical biosensor. *Nanotechnology* 25:205501
144. Xue L, Yamazaki H, Ren R, Wanunu M, Ivanov AP, Edel JB. 2020. Solid-state nanopore sensors. *Nat. Rev. Mater.* 5:931–51
145. Yamada H, Bandaru PR. 2016. Electrochemical kinetics and dimensional considerations, at the nanoscale. *AIP Adv.* 6(6):065325
146. Yang D, Liu X, Zhou Y, Luo L, Zhang J, et al. 2017. Aptamer-based biosensors for detection of lead(II) ion: a review. *Anal. Methhods* 9:1976–90
147. Yucesoy DT, Khatayevich D, Tamerler C, Sarikaya M. 2020. Rationally designed chimeric solid-binding peptides for tailoring solid interfaces. *Med. Devices Sens.* 3:e10065
148. Zhang Y, Ma R, Zhen XV, Kudva YC, Bühlmann P, Koester SJ. 2017. Capacitive sensing of glucose in electrolytes using graphene quantum capacitance varactors. *ACS Appl. Mater. Interfaces* 9:38863–69
149. Zhu Y, Guo F. 2013. Preparation and characterization of an unsupported nano-MoS2 catalyst. *Asian J. Chem.* 25:8057–60